Cellulose (2023) 30:11211–11230
https://doi.org/10.1007/s10570-023-05533-w

ORIGINAL RESEARCH

A synergistic self-cleaning and antibacterial studies of photocatalytic carbon nitride/polypyrrole coated cotton fabrics for smart textile application

Prathiba Meganathan · Lakshmi Manokari Selvaraj · Sounder Subbaiah · Venkatesh Subramanian · Sudhagar Pitchaimuthu · Nagarajan Srinivasan

Received: 29 June 2023 / Accepted: 27 September 2023 / Published online: 11 October 2023

Abstract Smart fabrics are one of the progressing technologies in this era especially in the field of self-cleaning and stain removing applications. Recent years, photocatalyst based self-cleaning technology seek much attention in the fields of therapeutic textiles, athletic clothing, defense uniforms and outdoor material. In this present work, the carbon nitride (CN) blended with conducting polypyrrole polymer (PPY) were coated over cotton fabrics by modified pad-dry cure method. The CNPPY composite coated cotton fabric shows enhanced photocatalytic degradation efficiency of 96.5% compared to individual coatings of CN and PPY. The successful demonstration of photocatalytic stain removal and self-cleaning properties was achieved through the utilization of CNPPY composite-coated cotton fabric. This breakthrough was accomplished with minimal water consumption (1 cm^2/ml), employing different colored stains under solar irradiation. Also, the CNPPY composite coated cotton fabric exhibited excellent resistance to bacterial growth. The dual advantages of photocatalytic antibacterial activity and self-cleaning of CNPPY composite coated cotton fabric led to sustainable, innovative textile applications with significant lower water consumption during washing process.

Keywords Photocatalyst · Smart textiles · Self-cleaning · Carbon nitride · Antibacterial activity

P. Meganathan (✉) · L. M. Selvaraj
Department of Textiles and Apparel Design, Periyar University, Salem, Tamilnadu, India
e-mail: prathiba@periyaruniversity.ac.in

S. Subbaiah
Department of Renewable Energy Science, Manonmaniam Sundaranar University, Tirunelveli, Tamilnadu, India

V. Subramanian
Department of Biotechnology, Manonmaniam Sundaranar University, Tirunelveli, Tamilnadu, India

S. Pitchaimuthu
Research Centre for Carbon Solutions, School of Engineering and Physical Sciences, Heriot-Watt University, Edinburgh EH14 4AS, UK

N. Srinivasan
Laboratory of Electrochemical Interfaces, Department of Chemistry, Manonmaniam Sundaranar University, Tirunelveli, Tamilnadu, India

Introduction

Today, the textile industry offers a vast and diverse range of fabrics that cater to a multitude of requirements and preferences. From natural fibers like cotton, silk, and wool, to synthetic materials such as polyester, nylon, and spandex, there is a fabric available for every purpose and occasion. These fabrics serve a multitude of applications, including clothing, home textiles, technical textiles, and industrial applications (Yetisen et al. 2016). Smart textile fabrics have been developed for various applications,

including anti-microbial (El-Nahhal et al. 2018), UV protection (Sricharussin et al. 2011), embedded sensor (Sedighi et al. 2014), Supercapacitors (Selvam and Yim 2023), Li Ion batteries (Praveen et al. 2021), hydrophobicity (Jeyasubramanian et al. 2016) and dye degradation (Baruah et al. 2019). In recent times, there has been a growing significance attributed to self-cleaning fabrics, which possess the remarkable ability to effectively remove dirt, stains, and other foreign substances from their surface. The development and utilization of self-cleaning textile fabrics offer a promising opportunity to decrease the reliance on surfactants during fabric washing, thereby contributing to the mitigation of water pollution (Ahmadi and Igwegbe 2018). Self-cleaning fabrics play a pivotal role in the textile industry today, as they significantly reduce both washing time and water pollution. One effective approach in the production of self-cleaning fabrics involves fabricating photocatalytic materials and coating them onto textile surfaces. The TiO_2 (Doganli et al. 2016; Fan et al. 2017; Hu et al. 2019; Özdemir et al. 2022), ZnO (Ji et al. 2022; Pal et al. 2018; Zhu et al. 2017), CuO(Sarwar, Bin Humayoun, Dastgeer and Yoon 2021), $BiVO_4$(Chen et al. 2022) and CuO (Vasantharaj et al. 2019), semiconductors coated fabrics were reported for the self-cleaning and dye degradation application. The anti-microbial properties of heterogeneous photocatalyst coated fabrics such as CuO/$BiVO_4$(Ran et al. 2019), Ag/ZnO/Cu (Hassabo et al. 2019), Ag–Cu_2O (Seth and Jana 2022), MnO_2/ZnO (Lam et al. 2021) , TiO_2/Ag (Hebeish et al. 2013), Cu(II)/TiO_2 (Yuzer et al. 2022) was investigated. The successful application of photocatalysts onto fabric surfaces is crucial for the development of self-cleaning fabrics. However, this process presents certain technical challenges that need to be overcome. Both direct and indirect methods of coating photocatalysts onto fabric have their limitations. One of the primary concerns is the effect of various parameters on the coating process. Factors such as coating temperature, solvent selection, and coating atmosphere can significantly influence the properties of the fabric. The temperature at which the coating is carried out needs to be carefully controlled to prevent any adverse effects on the fabric, such as changes in texture, color, or mechanical properties. Similarly, the choice of solvent plays a vital role in achieving uniform coating and avoiding damage to the fabric's structure. The coating atmosphere, including humidity and oxygen levels, can also impact the adhesion and stability of the photocatalyst coating. Another challenge lies in the limited range of light absorption exhibited by many photocatalysts. Traditionally, most photocatalysts primarily absorb ultraviolet (UV) light, which comprises only a small portion of the solar spectrum. This limited absorption range restricts the photocatalytic activity of the coated fabric to specific lighting conditions, such as direct exposure to UV light sources. To overcome this limitation, researchers have been exploring innovative approaches to enhance the light absorption capabilities of photocatalysts, particularly by expanding their absorption into the visible light range. Out of many visible light active photocatalyst, a Carbon Nitrite (CN) semiconductor has played an emerging role in many applications such as photocatalyst (Ong et al. 2016),s ensing (Idris et al. 2020), energy conversion and storage (Chen et al. 2016; Luo et al. 2019; Wang and Wang 2022). While CN is a well-known material for its broad light absorption spectrum, its photocatalytic activity is mostly restricted by photoelectron hole recombination (Zeng et al. 2018) and poorer charge transfer reaction at the surface (Chang et al. 2018), which limits its broader textile-related application. To overcome this issue, coating a conducting polymer as a co-catalyst over CN would enhance its photocatalytic efficiency (Meganathan et al. 2022). Polypyrrole (Wu et al. 2014) and polypyrrole blended metal oxide (Jain et al. 2017) semiconductors have been extensively studied and reported for various applications such as actuation (Liao et al. 2013), adsorbents (Feng et al. 2014), energy storage (Ma et al. 2015), electrocatalyst (Peng et al. 2012) and sensors (Wilson et al. 2012). In this study, we present an innovative approach involving the blending of carbon nitride (CN) with conducting polypyrrole polymer (PPY) to prepare a composite. This composite is subsequently applied as a coating onto cotton fabrics. The incorporation of a polypyrrole conducting polymer onto CN serves multiple purposes—it acts as a co-catalyst, a binder, reduces electron-hole recombination, and enhances charge transfer reactions. The resulting composite is anticipated to exhibit enhanced multifunctional properties, including efficient self-cleaning, stain removal, and resistance to bacterial growth when exposed to sunlight. The uniqueness of this composite-coated fabric significantly contributes to sustainability by reducing water consumption

during washing. The practical validation of its stain removal, self-cleaning, and antimicrobial properties heralds a transformation in the textile industry, promoting an environmentally friendly approach to fabric maintenance and longevity. To the best of our knowledge and literature survey, this is the first report on a CNPPY-based composite coating over cotton fabrics for photocatalytic self-cleaning in textile-based applications.

Experimental

Chemicals

The chemicals used in this study, namely Pyrrole ((C_4H_5N) 98%, Aldrich Chemical Co), Iron (III) Chloride ($FeCl_3$ anhydrous, powder, ≥ 99.99% trace metals basis), Urea (NH_2CONH_2) ACS reagent, (99–100%, average Mw ~ 534,000 by GPC powder), Rhodamine-B(RhB) ($C_{28}H_{31}ClN_2O_3$), Malachite green (MG) ($C_{23}H_{25}ClN_2$), Crystal violet (CV) ($C_{25}H_{30}N_3Cl$, ACS reagent, ≥ 90.0%), Methylene blue (MB)($C_{37}H_{27}N_3Na_2O_9S_3$) and polyvinylidene difluoride (PVDF) $–(C_2H_2F_2)_n–$ were used without purification. The study utilized 100% cotton (CT) fabric with Cambric Yarn count of 60s, warp per inch 120, weft per inch 80, warp to weft ratio 1:1, float density 9600, fabric weight 109 gms/Sqmts, and woven made construction, which was purchased from Varsha cotton mills private limited, Erode, Tamilnadu, India.

Carbon nitride (CN) was synthesized from urea using the thermal polymerization method, where the sample was heated up to 550 °C at a ramp rate of 15 °C min^{-1} and followed by maintain at the same temperature for another 2 h. The resulting yellow-colored flakes were collected after cooling. The PPY polymer was prepared using the oxidative chemical polymerization method, where 30 ml of 0.15 M pyrrole monomer was stirred at 0–5 °C, and 77 ml of 0.01 M $FeCl_3$ oxidant was added dropwise for 2 h. The dark-colored polymeric precipitate was then obtained and stored at 70 °C for 6 h.

CNPPY composite

The carbon nitride/polypyrrole (CNPPY) composite was synthesized through the oxidative chemical polymerization method. A 1 g of CN powder and 30 ml of 0.15 M pyrrole monomer were stirred for 2 h. Then, a 77 ml of 0.01 M $FeCl_3$ oxidant solution was gradually added at 0–5 °C temperature. The initial yellow mixture turned into a yellow with tinted grey colored solution. The obtained polymeric precipitate was washed with distilled water and stored at 70 °C for 6 h. The different molar concentrations of PPY were prepared (PPY 25, 50, 100, and 150 mM) over CN, and the photocatalytic dye degradation test used to identify the optimized CNPPY composite that exhibited superior photocatalytic activity. After confirming the optimized CNPPY concentration at 50mM, the composite was coated onto the cotton fabrics for further investigation.

CNPPY composites coated over cotton fabrics

For the incorporation of CNPPY over cotton fabrics (CNPPYCT), the modified pad dry cure method was employed. The CNPPY coating was mixed with PVDF binder and solvent in a ratio of 85:15 to obtain a homogeneous mixture using a mortar for 60 min. The coating process was carried out under controlled applied pressure of 3 bars. Subsequently, the coated fabrics dried at 80 °C for 5 min, followed by a curing at 120 °C for 3 min. The similar procedure was adopted for carbon nitride coated fabric (CNCT) and polypyrrole coated fabric (PPYCT).

Characterization technique

The surface morphology of materials CT, CNCT, PPYCT, and CNPPYCT was investigated by means of Fourier transform infrared (FT-IR) spectra of the composites, which were acquired using a powder sample technique with a spectral range of 400 to 4000 cm^{-1} employing a PerkinElmer FT-IR Spectrometer. For the SEM-EDX analysis, the samples were coated with a conductive material and imaged using a Carl Zeiss SEM-EDX. The UV–Vis diffused reflectance spectra were obtained by means of a spectrophotometer (Shimadzu UV-2700) using BaSO4 as the reflectance standard. The thermal stability of the samples was calculated under a ambient atmosphere using a thermogravimetric analyser (STA7200 HITACHI). X-Ray Photoelectron Spectrometer (Omicron Nano Technology, UK) was used to detect the chemical state of CT, CNCT, PPYCT and CNPPYCT was investigated.

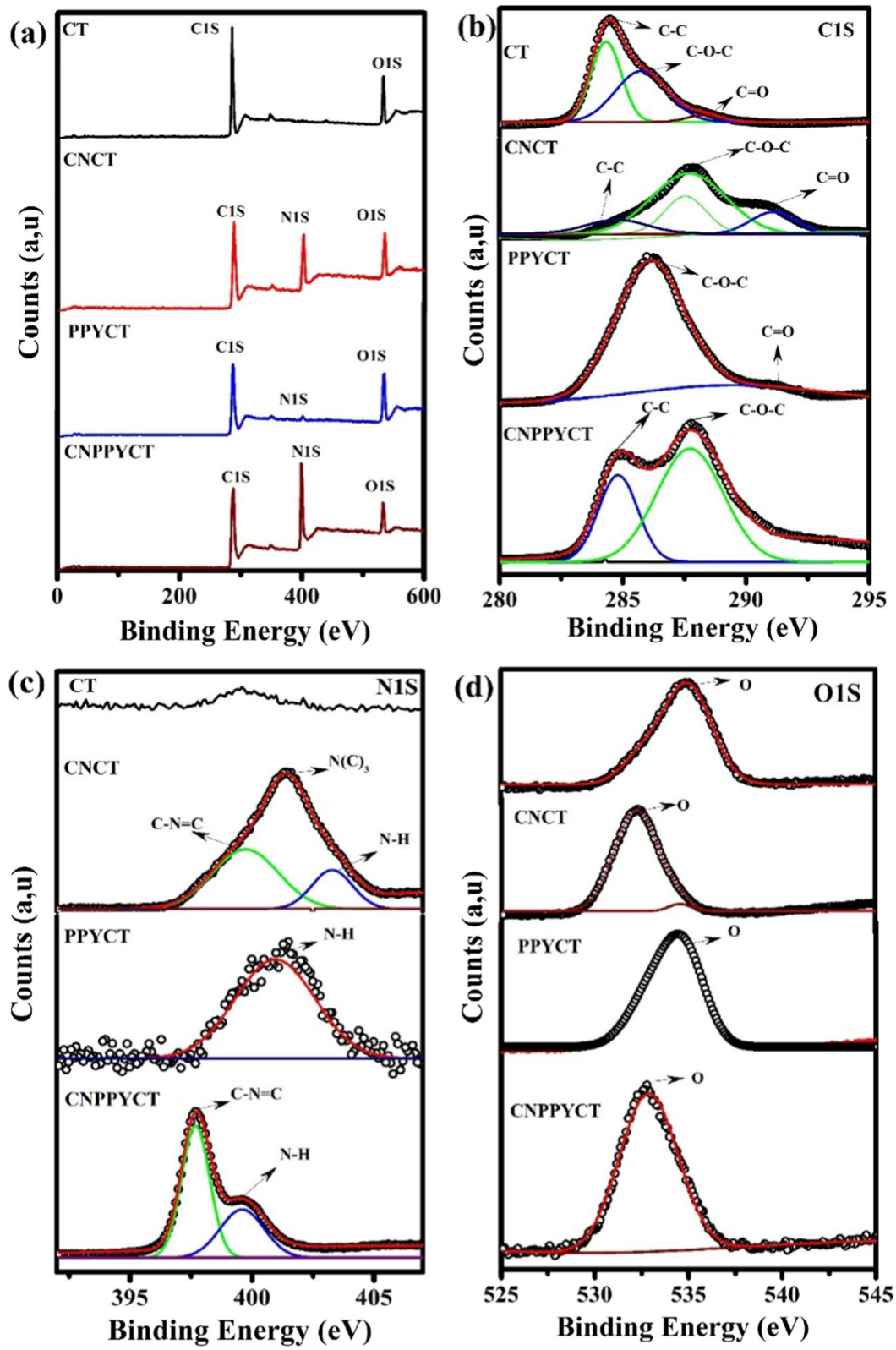
(a)
CT
C1S
O1S
CNCT
C1S
N1S
O1S
PPYCT
C1S
O1S
N1S
CNPPYCT
N1S
C1S
O1S
Counts (a,u)
0
200
400
600
Binding Energy (eV)
(b)
CT
C1S
C-C
C-O-C
C=O
CNCT
C-C
C-O-C
C=O
PPYCT
C-O-C
C=O
CNPPYCT
C-C
C-O-C
Counts (a,u)
280
285
290
295
Binding Energy (eV)
(c)
CT
N1S
CNCT
N(C)3
C-N=C
N-H
PPYCT
N-H
CNPPYCT
C-N=C
N-H
Counts (a,u)
395
400
405
Binding Energy (eV)
(d)
O
O1S
CNCT
O
PPYCT
O
CNPPYCT
O
Counts (a,u)
525
530
535
540
545
Binding Energy (eV)

◂**Fig. 1** XPS Spectrum of **a** survey spectra of uncoated CT, CNCT, PPYCT and CNPPYCT, **b** C1s spectra of uncoated CT, CNCT, PPYCT and CNPPYCT, **c** N1s spectra of uncoated CT, CNCT, PPYCT and CNPPYCT, and **d** O1s spectra of uncoated CT, CNCT, PPYCT and CNPPYCT

The Confocal Raman spectroscopy data was acquired by the WITec alpha-300R with a 785 nm laser wavelength. The laser beam was performed with the objective lens of 50X, and the light excited at the surface was composed into a spectrum by a diffraction grating 300 g/mm. The spectrum was recorded with a scan width and height of 50 µm and detected by a CCD camera.

Antibacterial studies

The antibacterial effectiveness of the textile samples was evaluated using the suspension test method in accordance with the guidelines outlined in the standard ISO 20743:2007, titled "Textiles - Determination of antibacterial activity of antibacterial finished products" with some modifications. To assess the photocatalytic antibacterial activity, wherein a bacterial suspension was directly inoculated onto the anti-bacterial coated cloth samples with broth. The coated cloth pieces were inoculated with a bacterial suspension containing 10^8*Escherichia coli* ATCC 25,922 bacterial cells. These samples, along with bacterial culture tubes, were separately placed under a solar stimulator and incubator (dark condition) for a 4-hour incubation period. The number of bacteria Colony-Forming Units (CFUs) was quantified using the colony plate count method. Viable bacterial cells were harvested through centrifugation, followed by serial dilution, and spread plating on Luria Bertani agar plates. After incubation at room temperature (37 °C) for 18 h, the plates were examined, and the colonies were counted, and their CFU values were recorded. (Hoefer and Hammer 2011; Hu et al. 2021; Meganathan et al. 2022)

The bactericidal rate (R %) was calculated to determine the percentage reduction of bacteria using the formula provided below Eq. (1), where NA and NB (CFU/ml) represented the number of colonies incubated under the solar stimulator and incubator, respectively.

$$R\,(\%) = \left[\left(N_B - N_A\right)/N_B\right] \times 100 \quad (1)$$

Photocatalytic experiments

The CT, CNCT, PPYCT, and CNPPYCT fabrics cut in to size of 5×5 cm were immersed in 1 × 10^{-4} M of RhB dye solution and kept in the dark for 1 h. After

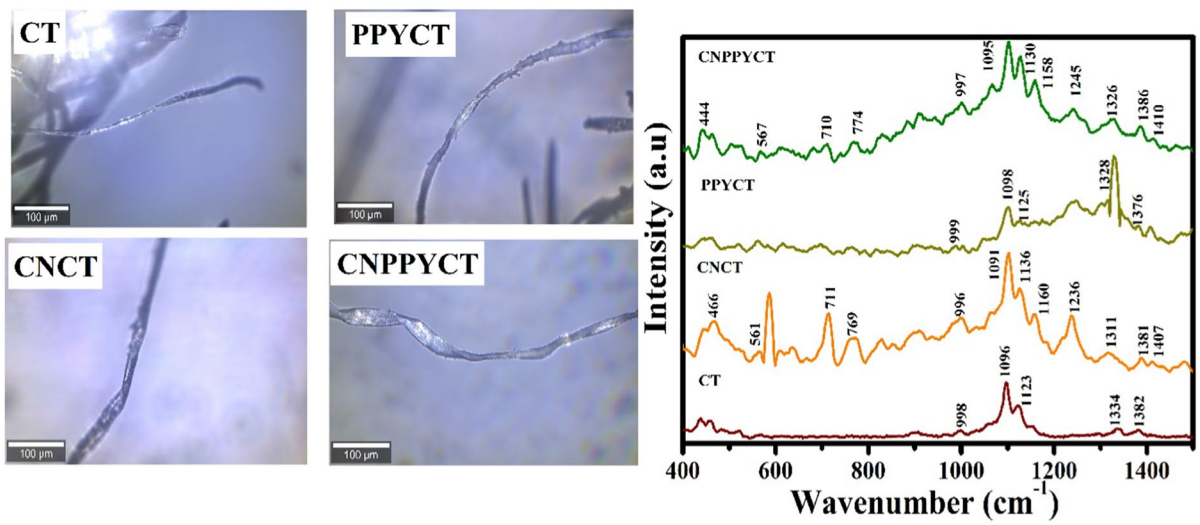

Fig. 2 Displays the Raman spectra and confocal image of CT, CNCT, PPYCT and CNPPYCT

that, the sample was irradiated using a solar simulator at room temperature. During the irradiation, absorbance studies were conducted at 30-minute intervals using 5 mL of RhB solution. The rate of variation in RhB concentration during each photocatalytic decolorization was monitored using a spectrophotometer at a wavelength of RhB at 554 nm.

The % removal of the dye was determined using the following Eq. (2) (Mahmoodi 2014) Where.

C_0 = Initial dye concentrations and C = Dye concentrations at time (t.)

$$\text{Percentage (\%) of dye removal} = C_0 - C/C_0 \times 100 \quad (2)$$

The photocatalytic self-cleaning property of CNPPY-coated fabrics was evaluated using various colored dyes as model stains, including RhB, Methyl Violet, Methylene Blue, and Malachite Green dyes. The fabrics were stained with different colored dyes, and their discoloration was tested under solar irradiation. Photographs were taken at 10-minute intervals to analyze the photocatalytic self-cleaning performance of the CNPPY-coated fabrics. To assess the washability and durability of the CNPPY-coated fabrics, it underwent a specific number of laundering cycles following a predefined experimental procedure reported by the literatures (Farouk et al. 2020; Gao et al. 2019). These parameters were meticulously chosen to achieve optimal outcomes in terms of both coating quality and overall performance.

Results and discussion

XPS analysis

The X-ray photoelectron spectroscopy (XPS) analysis results of the samples, consisting of uncoated cotton fabric (CT), carbon nitride coated cotton fabric (CNCT), polypyrrole coated cotton fabric (PPYCT), and carbon nitride/ polypyrrole coated cotton fabric (CNPPYCT), are presented in Fig. 1(a–d). In Fig. 1a, the wide-range XPS survey spectra reveal signals corresponding to C1s and O1s in CT (Wan et al. 2022), while CNCT, PPYCT, and CNPPYCT exhibit additional N1s signals, indicative of nitrogen moieties originating from the polymer (Singh et al. 2013) and carbon nitride (Tan et al. 2015). Figure 1b displays the deconvoluted high-resolution C1s XPS spectra of the samples. For CT, the C1s peak is resolved in C–C (284.5 eV), C–O (285.8 eV), and C=O (292.48 eV) (Jiang et al. 2018). In the case of PPYCT, the similar C–C peak (284.78 eV) obtained, the shifted C–O–C

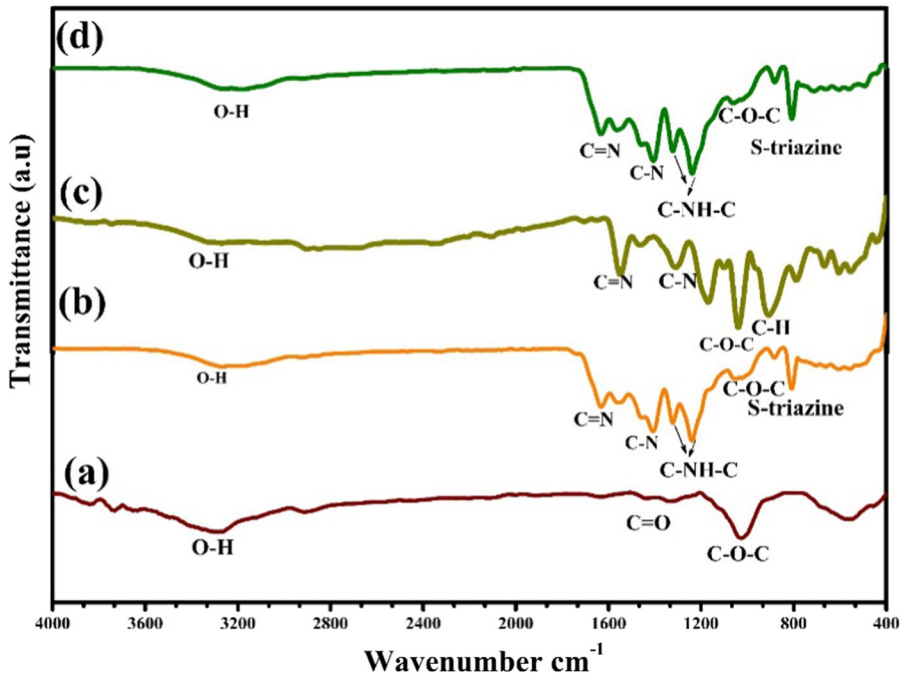

Fig. 3 FTIR Spectrum of **a** uncoated CT, **b** CNCT, **c** PPYCT and **d** CNPPYCT

(287.7 eV) and C=O (284.7 eV) peaks indicating an interaction between PPY's C–C group and the OH moieties of cellulose in the cotton fabric. Similarly CNCT displays new binding energies at (287.78, 290.58, and 294.18 eV), corresponding to C–C, C–O–C, and C=O, respectively, due to the interaction between CN and cellulose C and O moieties. The CNPPYCT shows peak shifts at C–C (284.85 eV) and C–O–C (287.7 eV) and reduced C–O peaks of cellulose, indicating an interaction between PPY's C–C group and the OH moieties of cellulose. Figure 1c presents the deconvoluted high-resolution XPS N1s spectra of the samples. The absence of an N1s peak in CT suggests the absence of nitrogen-containing moieties in cellulose. For CNCT, the N1s peak is deconvoluted into three peaks corresponding to C=N–C (399.18 eV), bridging N atoms in N–$(C)_3$ (401.14 eV), and N–H (403.28 eV) (Huang et al. 2019). The N1s peak of PPY displays characteristic peaks at 400.7 eV, attributed to positively charged nitrogen $–N^+–$. In the case of CNPPY-coated fabric, the two N1s fitting peaks are observed at 397.58 and 399.58 eV, corresponding to C=N–C and the peak of the neutral secondary amine structure –NH–. Figure 1d depicts the O1s spectra of the samples. The peaks observed in CT and PPYCT indicate the presence of C–O bonds. In PPYCT and CNPPYCT, peak shifts are observed, indicating the successful incorporation between PPY's C–C group and OH moieties in the cellulose matrix of cotton fabrics.

Raman analysis

Figure 2 Displays the Raman spectrum of CT, CNCT, PPYCT and CNPPYCT. The Raman spectrum of CT can be attributed to vibrations of cellulose molecule present in the cotton fibers. Notably, characteristic signals of cellulose are seen near 1123 cm^{-1} and 1096 cm^{-1}, corresponding to the C–C ring asymmetric stretching, C–O–C glycoside link symmetric stretching, and C–O–C glycoside link asymmetric stretching, respectively. Other noticeable bands are related to different types of CH_2 group vibrations, with peaks at 1382 cm^{-1} (scissoring) and 1334 cm^{-1}

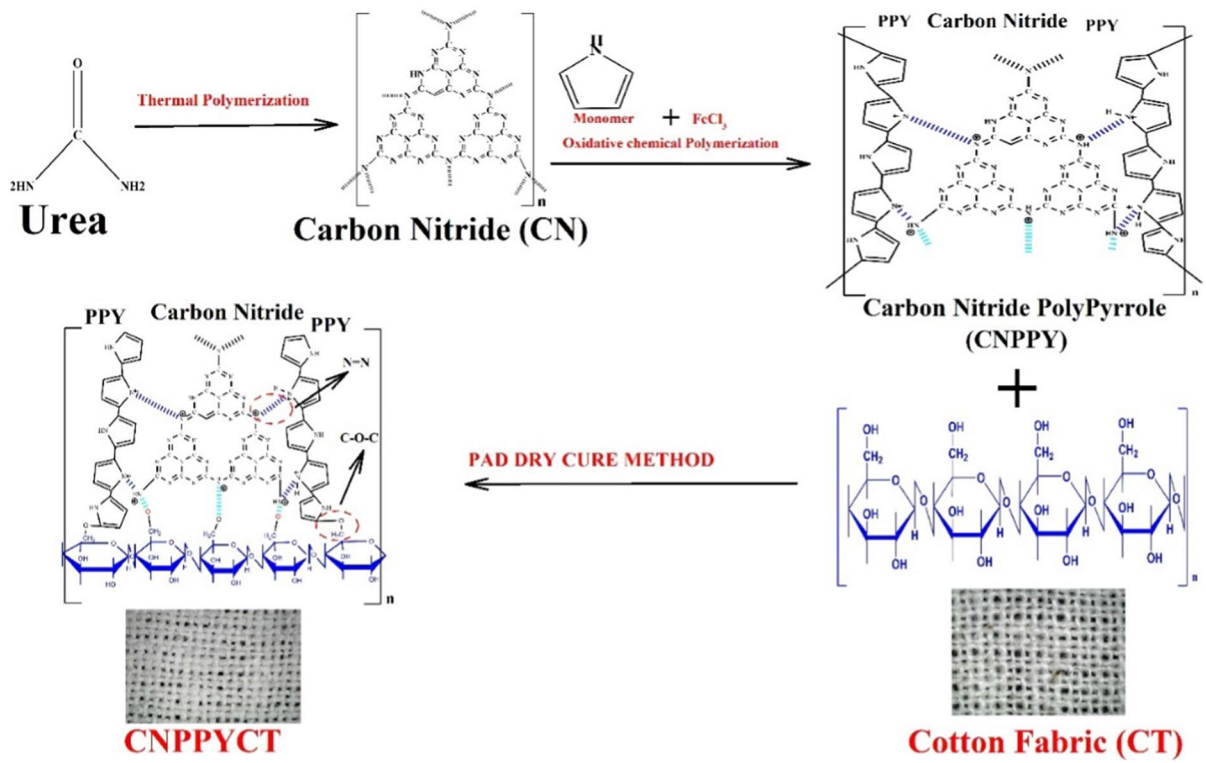

Fig. 4 Schematic depiction on interaction between CN, PPY and cotton fabric

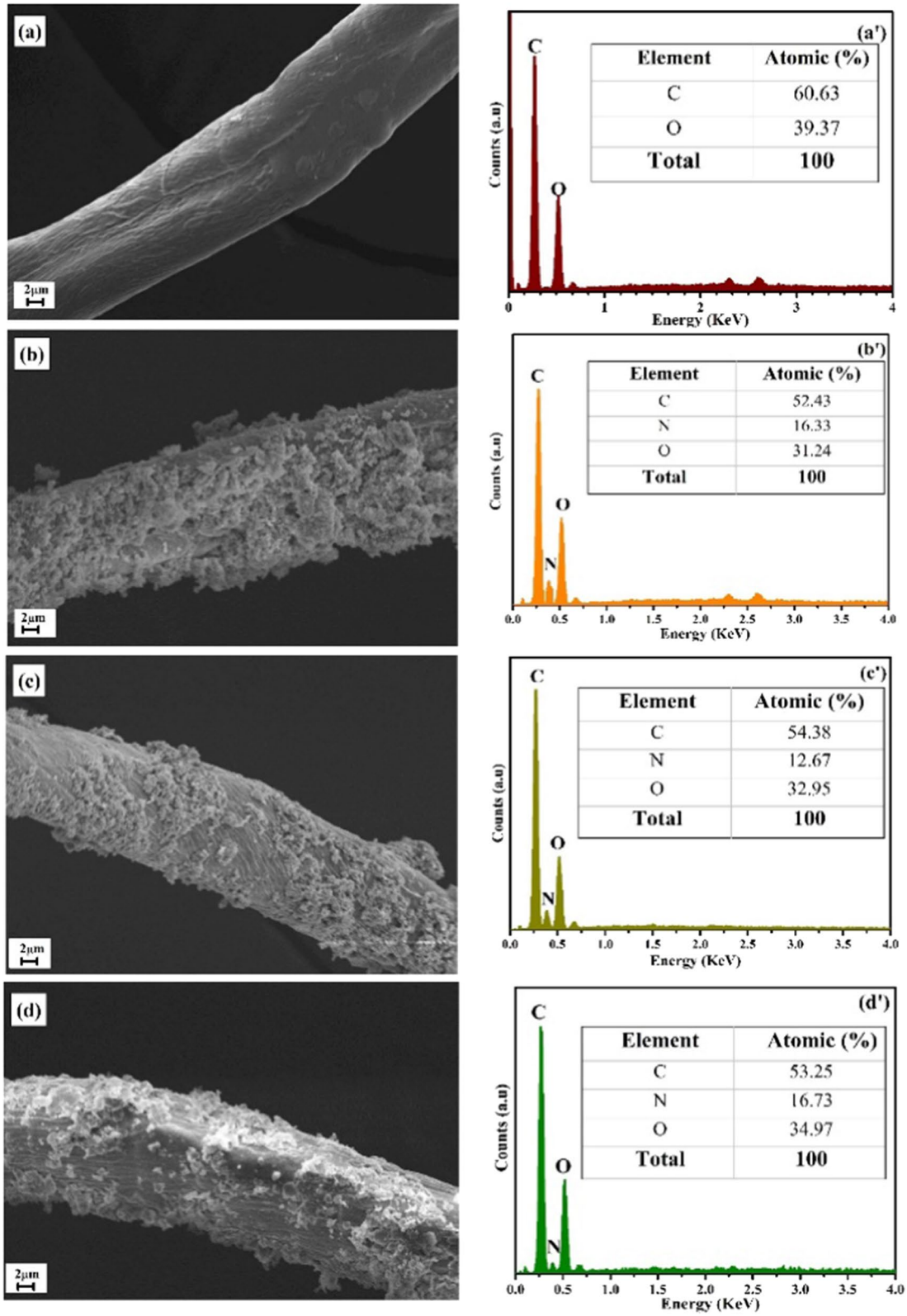
(a)
2μm
(a')
C
O
Element
Atomic (%)
C
60.63
O
39.37
Total
100
Counts (a.u)
Energy (KeV)
(b)
2μm
(b')
C
O
N
Element
Atomic (%)
C
52.43
N
16.33
O
31.24
Total
100
Counts (a.u)
Energy (KeV)
(c)
2μm
(c')
C
O
N
Element
Atomic (%)
C
54.38
N
12.67
O
32.95
Total
100
Counts (a.u)
Energy (KeV)
(d)
2μm
(d')
C
O
N
Element
Atomic (%)
C
53.25
N
16.73
O
34.97
Total
100
Counts (a.u)
Energy (KeV)

◂**Fig. 5** Scanning electron microscope and EDX analysis of (**a** and **a**') uncoated CT, (**b** and **b**') CNCT, (**c** and **c**') PPYCT and (**d** and **d**') CNPPYCT

(wagging involving scissoring of C–OH groups) along with rocking modes at 995 cm^{-1}.

The Raman spectra of carbon nitride (CN) coated on the cotton fabric exhibit multiple bands within the range of 700–1630 cm^{-1}, which are attributed to graphitic carbon nitride. Specifically, vibrations at 711, 996, 1160, 1236, and 1311 cm^{-1} are identified as the stretching vibrations of aromatic C-N heterocycles and various types of breathing modes of S-Triazine (Maślana, Kaleńczuk, Zielińska, and Mijowska, 2020). Moreover, the characteristic absorption peak at 1382 cm^{-1} corresponds to the stretching vibrations of the s-triazine ring (C_3N_3) units (Cao et al. 2016), while the peak at 1236 cm^{-1} is ascribed to the C (sp^2) bending vibration. Additionally, the peaks observed at 711, 769, 466, and 561 cm^{-1} are attributed to -heptazine-CN (Jiang et al. 2014). Furthermore, for PPYCT the vibrational bands in the vicinity of 1136, and 1091 cm^{-1} are indicative of cellulose's presence, associated with C–C ring asymmetric stretching, C–O–C glycoside link symmetric stretching, and C–O–C glycoside link asymmetric stretching, respectively. Other noticeable bands are related to different types of CH_2 group vibrations, with 1381 cm^{-1} corresponding to scissoring, and at 1311 cm^{-1}, wagging vibrations are accompanied by the scissoring of C–OH groups, followed by rocking modes at 996 cm^{-1}. These findings provide compelling evidence of the interaction and incorporation of CN over cotton fabric. For CNPPYCT in the spectrum of PPY, the peaks at 1552 and 1340 cm^{-1} arise from the π conjugated structure and ring stretching mode of the polymer backbone, respectively (Arteaga et al. 2013). The peak at 1037 cm^{-1} can be ascribed to the C–H in plane deformation, and the two faint peaks at 925 and 960 cm^{-1} correspond to ring deformation of the quinoid polaronic and bipolaronic structure, respectively. For the CNPPY-coated fabric, peaks at 999, 1130, and 1328 cm^{-1} correspond to PPY characteristic peaks of the ring deformation, C–H in-plane deformation, C–H in-plane bending, ring stretching, and C–C stretching, respectively. The peaks observed at 1376 cm^{-1} were attributed to symmetric and asymmetric C–H in- plane bending and C–N stretching modes, respectively. The Raman analysis corroborates the interaction and integration of carbon nitride (CN) and polypyrrole (PPY) onto the cotton fabric, aligning with the obtained XPS results.

FTIR analysis

The Fourier transform infrared (FTIR) spectra of uncoated cotton fabric (CT) and CT coated with carbon nitride (CN), polypyrrole (PPY), and the hybrid CNPPY are presented in Fig. 3(a–d). The pure CT spectrum in Fig. 3a displays absorption peaks at 3340, 2902, and 1023 cm^{-1}, corresponding to the OH, CH_2, and –C–O–C– stretching and bending vibrations in the cellulose matrix (Abd El-Hady et al. 2020; Himmelsbach et al. 2006; Yuen et al. 2012). A weak peak at 1638 cm^{-1} indicates the asymmetric stretching vibration of C=O, confirming the presence of cellulose in the cotton fabric (Himmelsbach et al. 2006). In Fig. 3b, the observed bands at 1240, 1320, and 1620 cm^{-1} represent the –C–NH–C, C=N, and C–N moieties in the carbon nitride structure, while the bands at 801 and 1403 cm^{-1} correspond to the s-triazine ring presence in the carbon nitride matrix (Shahbaz et al. 1984) (Gómez-Velázquez et al. 2023). The interactions between CN and the cotton fabrics are evident through broad bands between 1056 cm^{-1}, which is due to the C–O–C stretching vibrations in the cellulose matrix. For PPY (Fig. 3c, the peaks at 781, 918, 1315, and 1544 cm^{-1} confirm the presence of C–H, C=C, and C–N bonds, indicating PPY coating on the fabric. However, the red shifts observed from 1022 cm^{-1} (original PPY) to 1051 cm^{-1} suggest an interaction between the cellulose matrix and the PPY coating. These results align with previous findings in the literature (Varesano et al. 2013; Xie et al. 2019). In Fig. 3d, the predominant peaks at 781, 918, 1066, and 1315 cm^{-1} correspond to the C–H, C=C, C–O–C, and C–N bonds. The interactions between CN and the cotton fabrics are evident through broad bands between 1056 cm^{-1} is due to the C–O–C of cellulose matrix. The bands at 1234 and 1620 cm^{-1} confirm the presence of CN and PPY coated on the cotton fabrics.

Over all, the results obtained from XPS analysis (Fig. 1), Raman spectroscopy (Fig. 2), and FTIR (Fig. 3) presented a coherent narrative of the interactions between the CN, PPY, and cellulose matrix. From the above confirmation, the bonding

interactions between CN, PPY, and cotton fabrics were illustrated in Fig. 4.

Morphological analysis

The scanning electron microscopic (SEM) images of uncoated and photocatalyst-coated cotton fibers are presented in Fig. 5(a–d). The images in Fig. 5(b, c, and d) demonstrate that the fibers of the cotton fabric are coated with CN, PPY, and CNPPY composite materials. These results validate the efficacy of the modified pad dry cure method in successfully coating pre-synthesized photocatalyst materials onto the fabric fibres. The Fig. 5(a'–d') showcases the Energy Dispersive X-ray (EDAX) elemental peaks, specifically for carbon, oxygen, and nitrogen, which are in direct correlation with the presence of polypyrrole (PPY), carbon nitride (CN), and the hybrid CNPPY coatings on the cotton fabrics. This compelling evidence firmly establishes the successful deposition of PPY, CN, and CNPPY layers on the fabric surfaces, validating the efficacy of the coating process.

Optical analysis

Figure 6 displays the optical absorbance spectra of CT, PPYCT, CNCT, and CNPPYCT. It is evident that CT and PPYCT do not exhibit any light absorption behavior in the UV and visible regions. However, CNCT shows effective light absorption between the 300–550 nm region. Furthermore, the CNPPYCT composite noticeably shifts the light absorbance range a few nanometers towards the visible region. These results confirm that CNCT and CNPPYCT can be utilized for photocatalytic activity under natural sunlight.

The band gaps of CNCT and CNPPYCT were calculated using Tauc's plot, as shown in Fig. 7. The calculated band gap values of CNCT and CNPPYCT are 2.82 and 2.81 eV, respectively, which are consistent with previously reported literature (Wang et al. 2009).

Thermal analysis

The Thermo gravimetric analysis (TGA) presented in Fig. 8. it provides the thermal changes occurring in CT, PPY, CN, and CNPPY composite coated cotton fabric. The TGA profile of CT shows 11% weight reduction at 120 °C, which was likely caused by the elimination of moisture content. Starting at 250 °C the thermal decomposition peak gradually begins to occur and decompose significantly at 250 °C. At the maximum melting point at 375 °C a 100% decomposition was reached for cotton fabric (Krishnamoorthy et al. 2012). The TGA of PPY shows a weight loss in three stages. The first stage is range of 30 and 170 °C and shows about 11% reduction in weight. This may correspond to loss adsorbed moisture and bounded solvent. The second stage of weight loss at 170° C and continued at 320 °C during which there was a 61% of weight loss due to the degradation of cotton fabric and residual organic solvent/pyrrole monomer (Boukoussa et al. 2017). The third stage of weight loss starts at 320 °C and continues to up 550 °C during which there was a 28% of weight loss due to the complete degradation of PPY polymer matrix. The CNCT sample showed an approximate mass reduction of 14%, while the CNPPYCT sample exhibited a slightly lower reduction of around 8%. These mass reductions can be attributed to the removal of hydrogen from the carbon nitride and cotton fabrics, respectively. As the temperature increased within the range of 370 to 400 °C, another notable transformation took place. The α-cellulose present in the cotton fabrics underwent degradation, which refers to the process of breaking down large polymer chains into smaller units (Shahedifar and Rezadoust 2013). This degradation resulted in the formation of aliphatic char, which subsequently converted into aromatic structures. During this process, water, methane, carbon monoxide, and carbon dioxide were released. As a result, the CNPPYCT sample exhibited a better flame-retardant properties due to the minimal generation of flammable gases and a low decomposition rate. This indicates its improved ability to resist combustion compared to the CNCT sample, making it suitable for intended to specific flame resistance applications (Xu et al. 2017).

Photocatalytic studies

The degradation of Rhodamine-B (RhB) dye under light irradiation for 120 min was investigated, and the optical absorbance of RhB dye measured at different time intervals with CT, PPY, CN and CNPPY are presented in Fig. 9(a, b, c, and d). The optical absorbance spectra of CT indicate a minor decrease

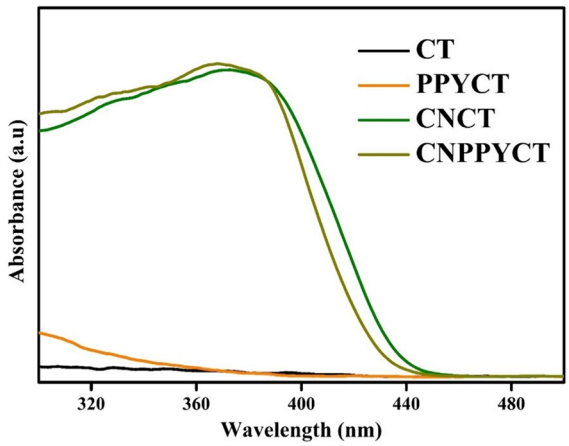

Fig. 6 UV-Visible absorption spectrum of uncoated cotton fabric (CT) and photocatalyst materials (CN, PPY and CNPPY composite) coated cotton fabric

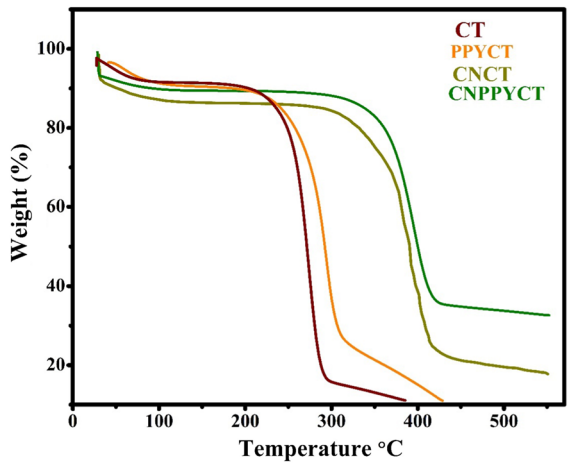

Fig. 8 The Thermo gravimetric analysis (TGA) of CT, PPY, CN, and CNPPY composite coated cotton fabric

in the absorption spectrum corresponding to the RhB dye adsorbed over the surface of CT, but there is no photocatalytic dye degradation. In contrast, PPYCT shows higher dye adsorption tendency than the pure cotton fabrics due to the interactions between dye molecules and PPY, but the degradation efficiency of PPYCT is almost negligible after light irradiation. Before light irradiation, the CNCT and CNPPYCT show strong RhB dye adsorption, indicating the existence of a larger surface area over the cotton fabric by CN and PPY.

After light irradiation, the amount of RhB dye molecules slowly decreases due to the photodegradation of dye molecules. A hypochromic shift is observed at 554 nm after 60 min of light irradiation in Fig. 9(c and d), indicating the residues of photodegraded dye molecules and the formation of its intermediates (Cui et al. 2015). The above results demonstrate that CNPPYCT exhibits excellent photocatalytic activity compared to CNCT, PPYCT, and CT.

The C/C_0 vs. time plots shows the calculated concentration changes over time of a RhB dye in Fig. 10a. The results indicate that the CNPPY composite coated cotton fabric exhibited the highest photocatalytic dye degradation efficiency of 96.5%, which is significantly higher than that of the

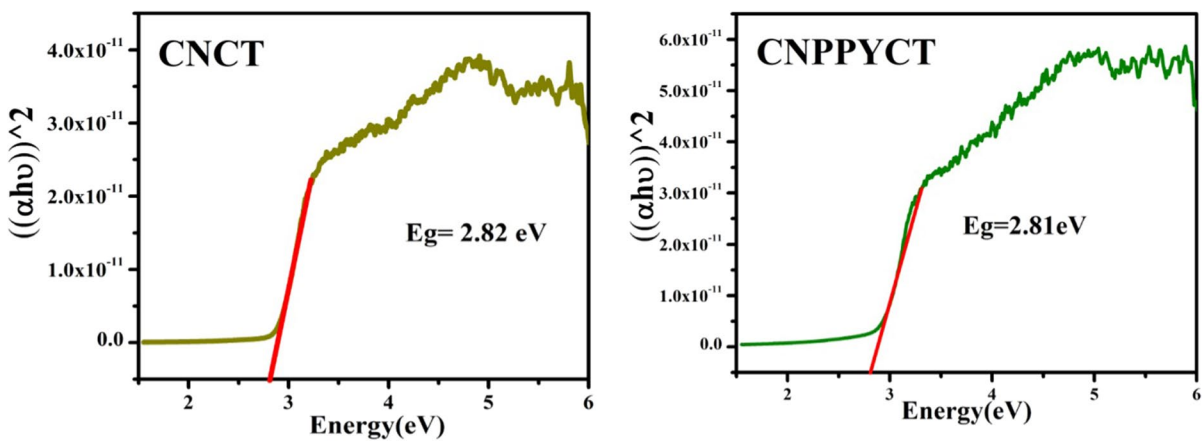

Fig. 7 The tauc plot of CNCT and CNPPYCT

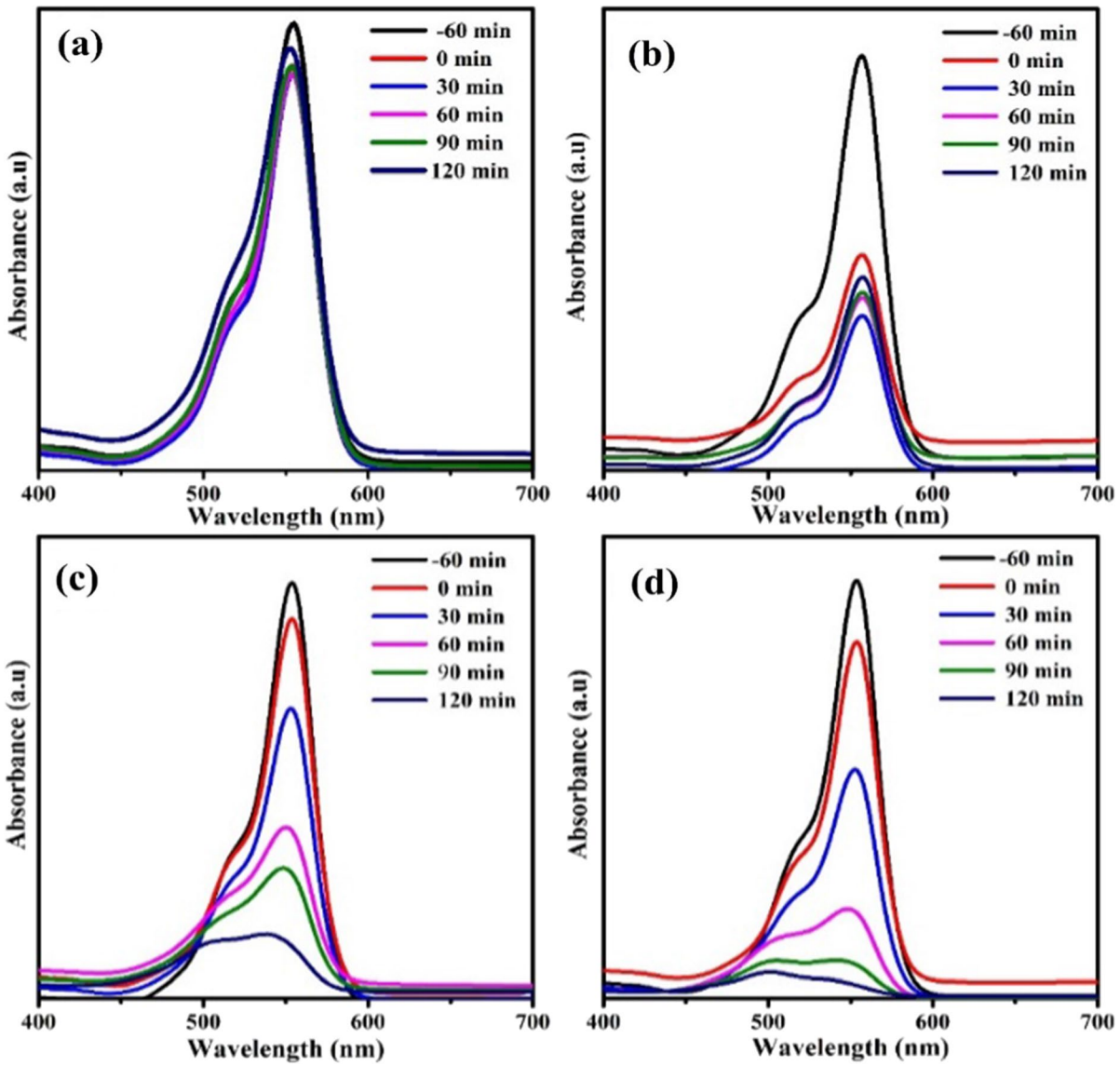

Fig. 9 Photocatalytic degradation of RhB solution over of **a** uncoated CT, **b** PPYCT, **c** CNCT and **d** CNPPYCT

individual CN (87%) and PPY (58%) coatings over the cotton fabrics. The superior photocatalytic activity of CNPPY composite can be attributed to several factors, including the broadening of the light-harvesting region, which promotes photocharge carrier generation and accelerates the photocatalysis reaction rate; the enhanced dye adsorption rate by PPY through π–π* interactions; and the high charge separation at the CNPPY hetero interfaces, which significantly lowers the recombination rate (Ovando-Medina et al. 2018). The photodegradation efficiency of CT, PPYCT, CNCT and CNPPYCT coated fabrics was calculated and is shown in Fig. 10b. The results clearly show that the degradation level of CNPPYCT reaches 96.5% after 120 min of photocatalytic reaction, while it was 0, 58, and 87% for CT, PPYCT, and CNCT respectively. The photocatalytic activities of the coated cotton fabrics follow the order CNPPYCT > CNCT > PPYCT > CT.

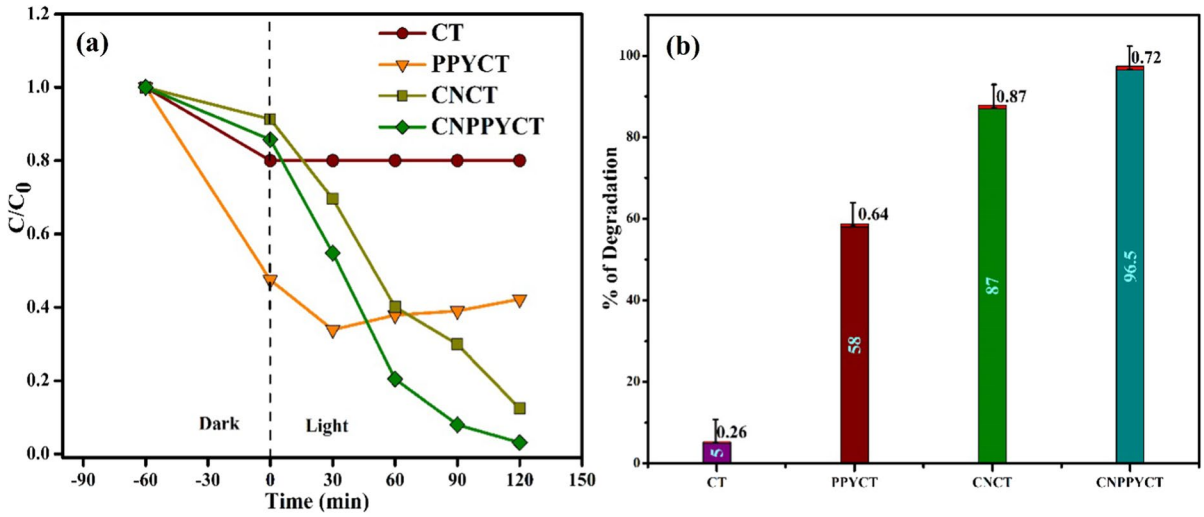

Fig. 10 **a** C/C_0 vs. time plot and **b** Photocatalytic degradation efficiency (%) of uncoated CT, CNCT, PPYCT and CNPPYCT

Photocatalytic dye degradation reaction pathways

The surface of CNPPY absorbs light energy when exposed to sunlight light. The photo excited electrons are generated from the valence band (VB) of CN and PPY migrated to the conduction band (CB) of CN and PPY, producing electron-hole pairs in Eq. (3). A photo-induced electrons generated from the conduction band (CB) of PPY migrated to the conduction band (CB) of CN across the heterointerface because the conduction band (CB) of PPY is higher than that of CN. At the junction, the PPY promotes this photo-excited charge transport and serves as to prevent the recombination reaction of photoinduced electrons from the CN. According to Eq. (4) the photo generated holes from the valence Band (VB) react with water to produce OH^- radical. And also, the electron in the conduction (eCB) is taken up by the surrounding (O_2) molecule and produce anionic superoxide radicals (O_2^{*-}) shown in Eq. (5). These generated superoxides radical (O_2*-) reacts with the hole (CNPPYCT h+) to produce a peroxyl radical (HO_2*) in Eq. (6). The generated peroxyl radical (HO_2*) from Eq. (6) reacts with a photoexcited electron (e−) to convert into a negatively charged peroxyl radical (HO_2^-) (Eq. 7). The negatively charged peroxyl radical (HO_2^-) reacts with a positively charged hole (h+) to form hydrogen peroxide (H_2O_2) (Eq. 8). These Hydrogen peroxide (H_2O_2) reacts with a photoexcited electron (e−) to produce a hydroxyl radical (OH*) (Eq. 9). Finally The dye molecule (RhB) reacts with the hydroxyl radical (OH*) to undergo degradation, resulting in the formation of intermediate organic fragments compounds, carbon dioxide (CO_2), and water (H_2O) (Eq. 10) (Ajmal et al. 2014).

$$\text{CNPPYCT} + h\upsilon \rightarrow \text{CNPPYCT}\, h^+ + \text{CNPPYCT}\, e^- \quad (3)$$

$$\text{CNPPYCT}\, h^+ + H_2O \rightarrow H^+ + OH^- \quad (4)$$

$$\text{CNPPYCT}\, e^- + O_2 \rightarrow O_2^{*-} \quad (5)$$

$$O_2^{*-} + \text{CNPPYCT}(h^+) \rightarrow HO_2^* \quad (6)$$

$$HOO^* + e^- \rightarrow HO_2^- \quad (7)$$

$$HO_2^- + h^+ \rightarrow H_2O_2 \quad (8)$$

$$H_2O_2 + e^- \rightarrow OH^* + OH^- \quad (9)$$

$$\text{RhB} + OH^* \rightarrow \text{Intermediate} + \text{Minerals} + CO_2 + H_2O \quad (10)$$

Photocatalytic self-cleaning analysis

The investigation of the self-cleaning property of CNPPY coated fabrics involved using various colored

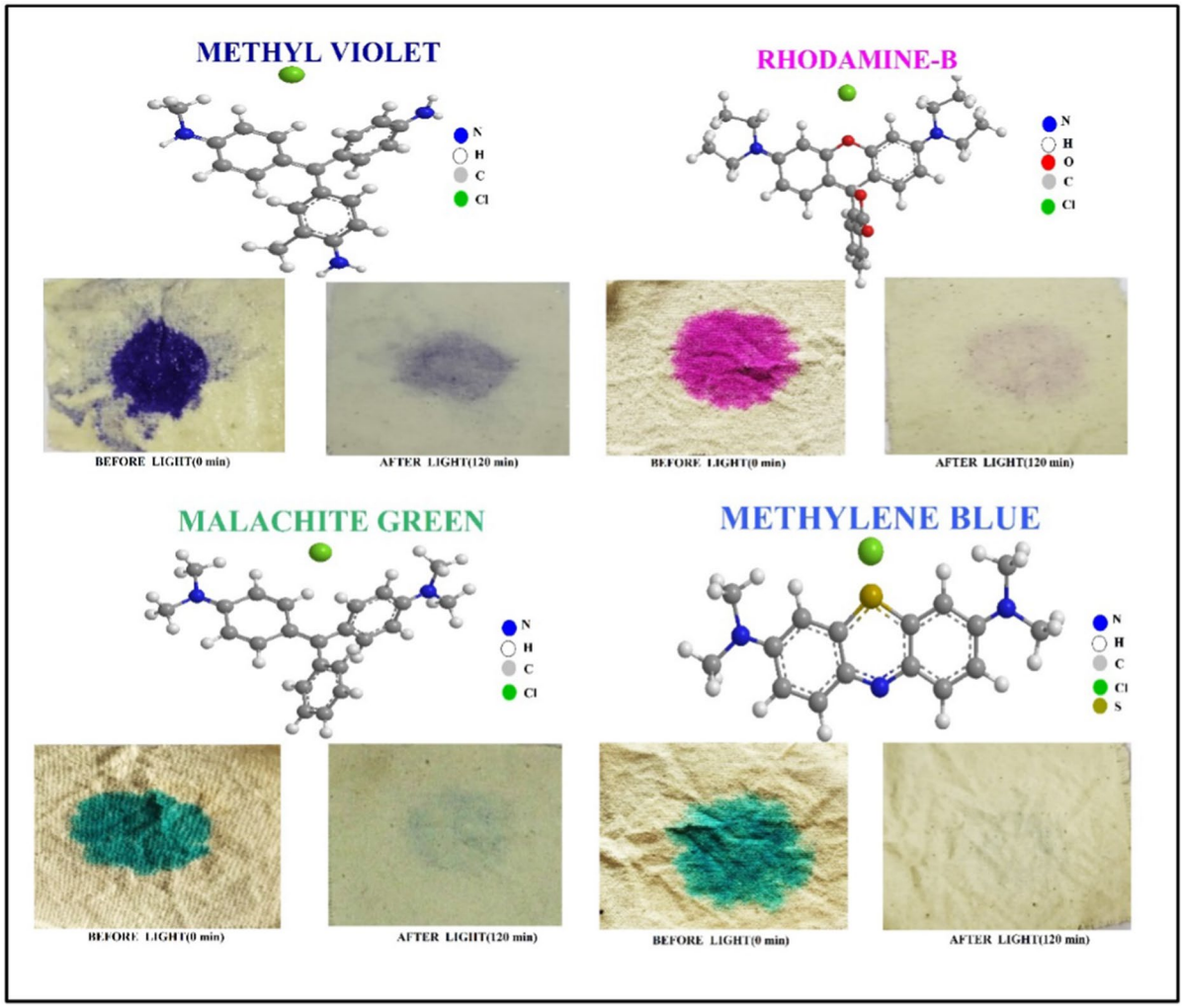

Fig. 11 Self-cleaning and stain removal activity demonstration of CNPPY coated cotton fabrics before and after 2 h solar irradiation

dyes as model stains, which were kept under simulated solar irradiation for 2 h. As shown in Fig. 11, the colored dye-stained fabrics changed from their respective colors to colorless under light irradiation, indicating that the CNPPY coated fabrics have self-cleaning activity and the colored dye stains are removed by the photocatalytic process. It is noteworthy that the photocatalytic self-cleaning experiment over coated cotton fabrics consumed less amount of water (1 cm^2/ml) compared to conventional photocatalytic powder type experiments (Ahmad et al. 2021; Duraimurugan et al. 2020). This suggests that the photocatalyst coated cotton fabric reduces water consumption, and less use of surfactant in the stain removal process might significantly reduce water pollution.

Photocatalytic self-cleaning mechanism

A photocatalytic mechanism for the self-cleaning and stain removing process over cotton fabric surface was proposed. The plausible photocatalytic self-cleaning mechanism are illustrated in Fig. 12. When light is irradiated on the CNPPY composite, photoexcited electrons and holes are generated at the conduction band (CB) and valence band, respectively. The photoexcited electrons generated from the conduction bands (CB) of CNPPY leads to the production of superoxide radicals ($\cdot O_2^-$) with a water molecule.

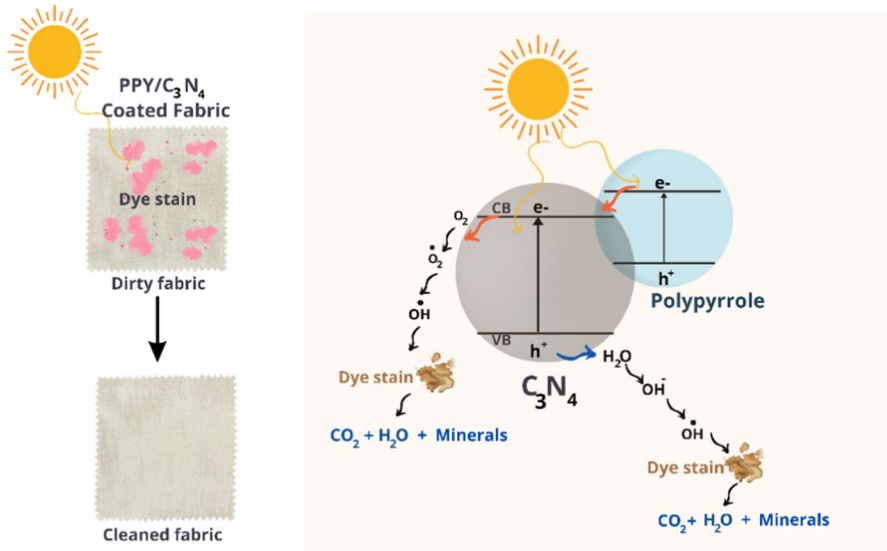

Fig. 12 Mechanism of photo catalytic stain removal under solar irradiation

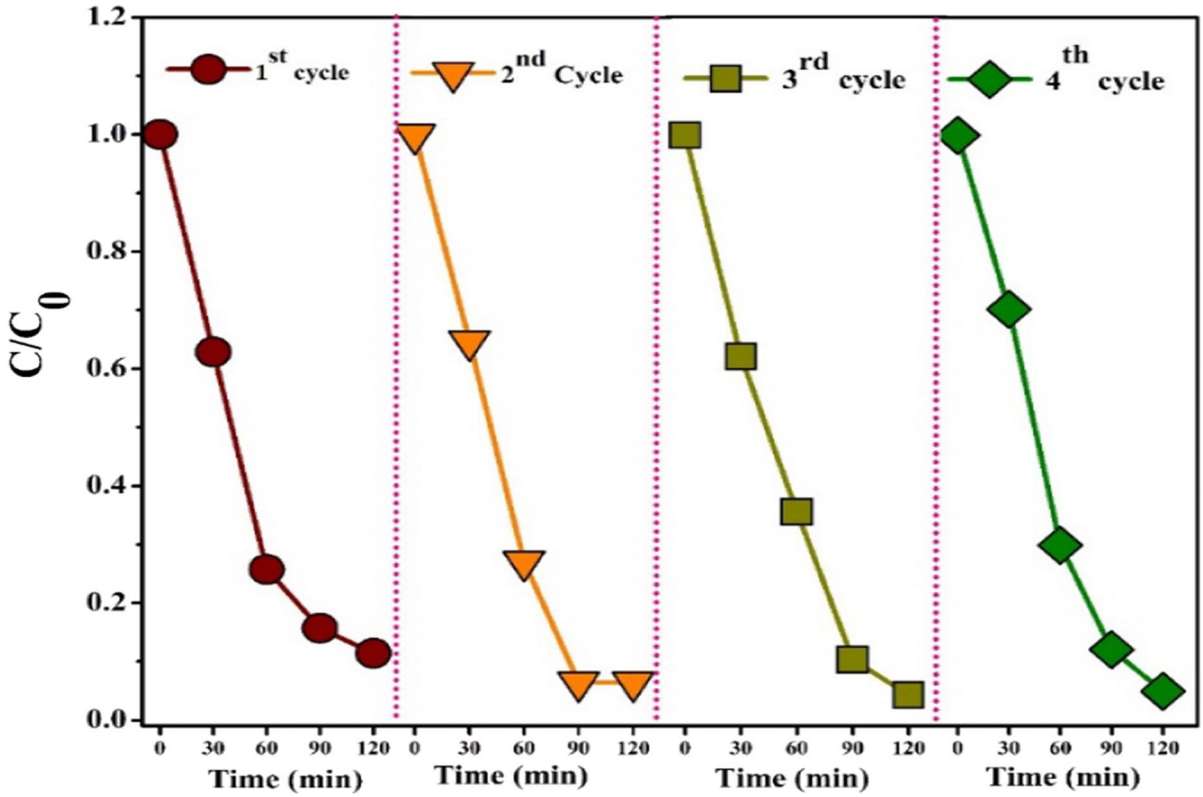

Fig. 13 Cyclic stability of CNPPYCT under four consecutive cycles

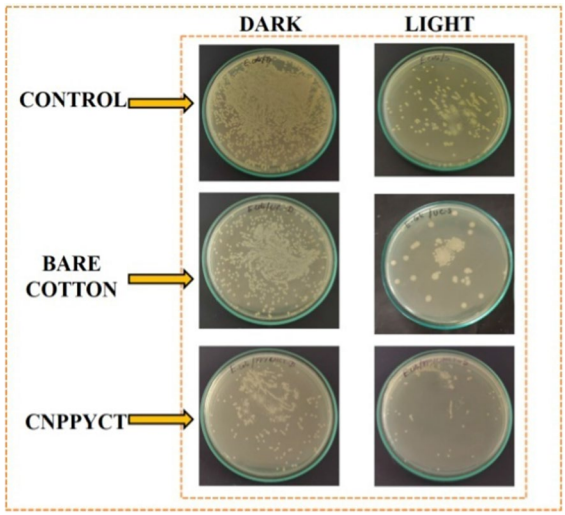

Fig. 14 Antimicrobial activity of Control, uncoated CT and CNPPYCT

These photogenerated superoxide radicals degrade the dye/stain molecules into minerals and CO_2. On the other hand, the photo-generated holes at the valence band (VB) of CNPPY are produce hydroxyl radicals ($\cdot OH^-$) from a water molecule. These hydroxyl radicals effectively oxidize the dye/stain molecules into CO_2 and minerals. Earlier reports (Kang et al. 2015) and (Franco 2020) showed that the CNPPY interfaces form a type-II band alignment, which supports a feasible photoexcited electrons and holes transfer reaction.

Photocatalytic reusability assessment

In Fig. 13, the CNPPYCT reveals that there is no significant photodegradation efficiency loss for four cycles. The recyclability test was able to understand that the CNPPY composite was firmly attached to the cotton fabric and are stable for photocatalytic self-cleaning application for longer life cycle.

Photocatalytic antimicrobial analysis and mechanism

To assess the antimicrobial efficacy of the coated fabric, the bacterial growth inhibition was evaluated using the colony count method(CFU) (Fig. 14). The results demonstrate that the CNPPYCT composite exhibits highly effective resistance against Gram-negative bacterium *Escherichia coli* ATCC 25,922 when compared to CN and PPY coatings. The CFU/ml values of Escherichia coli are listed in Table 1. When in contact with a bacterial suspension or contaminated surface, the CNPPYCT coating attracts bacteria through van der Waals forces and other weak interactions. Upon exposure to light, the photocatalyst in CNPPYCT absorbs photons and generating photoexcited electron-hole pairs. The photo-generated electron-hole pairs in the conduction band (CB) and valance band (VB) become highly reactive, leading to the production of various ROS, primarily hydroxyl radicals ($\cdot OH$) and superoxide radicals ($\cdot O_2$-). These ROS act as strong oxidizing agents, causing damage to bacterial cells by disrupting their membranes, lipids, proteins, and DNA. The oxidative effect of hydroxyl radicals penetrates the bacterial cell walls, leading to the loss of cell membrane and wall integrity and the degradation of essential biomolecules, ultimately resulting in bacterial cell death. The photocatalytic process continues as long as there is light and the presence of the photocatalyst, ensuring a sustained antibacterial effect (Abbas et al. 2016; Ekande and Kumar 2021).The mechanism of photocatalytic

Table 1 CFU values of bacteria control and photo catalytic compounds coated cloth

S. no.	Particulars	Average bacterial count (1×10^8)		Bactericidal rate (%)	
		Absence of light	Presence of light	Absence of light	Presence of light
1.	Control (Uncoated Fabric)	332	34	–	–
2.	Cotton fabric (CT)	270	33	18	3
3.	CN coated fabric (CNCT)	67	29	79	14
4.	CNPPY coated fabric (CNPPYCT)	49	13	85	63

reactive species generation by the action of natural irradiation was clearly described using Eqs. (3–10 and 11). These findings suggest that the CNPPY composite-coated cotton fabric possesses significant antimicrobial activity against *Escherichia coli.*

$$2OH^{*} + \textit{Escherichia coli} \rightarrow \text{Intermediate} + \text{Minerals} + CO_2 + H_2O^{-} \quad (11)$$

Conclusion

The CN and PPY composite were synthesized using oxidative chemical polymerization, and a modified pad dry cure method was employed to coat the cotton fabrics with PPY, CN, and CNPPY. Elemental analysis and XPS, RAMAN and FTIR studies confirmed the interaction of PPY and CN on the cotton fabrics (CT). The addition of PPY to the CN-coated fabric resulted in improved photodegradation efficiency, stability, and reusability. Furthermore, the CNPPY composite-coated fabrics exhibited excellent photocatalytic self-cleaning properties and antimicrobial activity. A minimal water consumption of 1 cm^2/ml was validated through a photocatalytic self-cleaning test. This study presents a promising avenue for the advancement of smart textiles that integrate photocatalytic self-cleaning. The implementation of this technology could potentially lead to reduced water and surfactant usage, thus contributing to the mitigation of water pollution.

Acknowledgments The author SN would like to acknowledge the Tamilnadu State Government Higher Education (H2) Department is gratefully acknowledged for the establishment of the Central Instrument Facility (GO (Ms) No. I59) and DST-FIST Project (SR/FST/CSI – 247/2012) for their infrastructure support.

Author contributions PM: Investigation, Formal analysis, Methodology, Writing—original draft. SS: Formal analysis, Data curation, Writing—review & editing. LMS: Investigation, Formal analysis, Methodology, Data curation. VS: Data curation, Writing—review & editing. SP: Formal analysis, Data curation, Writing—review & editing. NS: Conceptualization, Methodology, Validation, Data curation, Supervision, Writing—review & editing, Funding acquisition.

Funding Not applicable.

Data Availability The datasets generated during and analyzed during the current study are available from the corresponding author on reasonable request.

Declarations

Conflict of interest The authors have no conflicts of interest to declare that are relevant to the content of this article.

Ethical approval Not applicable.

References

Abbas N, Shao GN, Haider MS, Imran SM, Park SS, Jeon S-J, Kim HT (2016) Inexpensive sol-gel synthesis of multiwalled carbon nanotube-TiO_2 hybrids for high performance antibacterial materials. Mater Sci Eng C 68:780–788. https://doi.org/10.1016/j.msec.2016.07.036

Abd El-Hady M, Sharaf S, Farouk A (2020) Highly hydrophobic and UV protective properties of cotton fabric using layer by layer self-assembly technique. Cellulose 27:1099–1110. https://doi.org/10.1007/s10570-019-02815-0

Ahmad M, Rehman W, Khan MM, Qureshi MT, Gul A, Haq S, Menaa F (2021) Phytogenic fabrication of ZnO and gold decorated ZnO nanoparticles for photocatalytic degradation of rhodamine B. J Environ Chem Eng 9(1):104725. https://doi.org/10.1007/s10570-019-02815-0

Ahmadi S, Igwegbe CA (2018) Adsorptive removal of phenol and aniline by modified bentonite: adsorption isotherm and kinetics study. Appl Water Sci 8(6):1–8. https://doi.org/10.1007/s13201-018-0826-3

Ajmal A, Majeed I, Malik R, Idriss H, Nadeem M (2014) Principles and mechanisms of photocatalytic dye degradation on TiO_2 based photocatalysts: a comparative overview. RSC Adv 4:37003–37026. https://doi.org/10.1039/C4RA06658H

Arteaga G et al (2013) Nucleation and growth mechanism of electro-synthesized poly (pyrrole) on steel. Int J Electrochem Sci 8(3):4120–4130. https://doi.org/10.1016/S1452-3981(23)14458-0

Baruah B, Downer L, Agyeman D (2019) Fabric-based composite materials containing ZnO-NRs and ZnO-NRs-AuNPs and their application in photocatalysis. Mater Chem Phys 231:252–259.

Boukoussa B, Abidallah F, Abid Z, Talha Z, Taybi N, Hadj SE, Bengueddach H (2017) Synthesis of polypyrrole/Fe-kanemite nanocomposite through in situ polymerization: effect of iron exchange, acid treatment, and CO_2 adsorption properties. J Mater Sci 52(5):2460–2472

Cao Y et al (2016) Monolayer gC_3 N_4 fluorescent sensor for sensitive and selective colorimetric detection of silver ion from aqueous samples. J Fluoresc 26:739–744. https://doi.org/10.1007/s10895-016-1764-9

Chang F, Zheng J, Wang X, Xu Q, Deng B, Hu X, Liu X (2018) Heterojuncted non-metal binary composites silicon carbide/g-C_3N_4 with enhanced photocatalytic performance. Sci Semicond 75:183–192. https://doi.org/10.1016/j.mssp.2017.11.043

Chen X, Liu Q, Wu Q, Du P, Zhu J, Dai S, Yang S (2016) Incorporating graphitic carbon nitride (g-C_3N_4) quantum dots into bulk-heterojunction polymer solar cells leads to efficiency enhancement. Adv Funct Mater 26(11):1719–1728. https://doi.org/10.1002/adfm.201505321

Chen J, Li H, Bai X, Wang C, Liu S, Song X (2022) Situ preparation of $BiVO_4$ functionalized cotton fabric for ultraviolet protection and self-cleaning properties. Integr Ferroelectr 227(1):246–256. https://doi.org/10.1080/10584587.2022.2065591

Cui Y, Goldup SM, Dunn S (2015) Photodegradation of rhodamine B over Ag modified ferroelectric BaTiO 3 under simulated solar light: pathways and mechanism. RSC Adv 5(38):30372–30379. https://doi.org/10.1039/C5RA00798D

Doganli G, Yuzer B, Aydin I, Gultekin T, Con AH, Selcuk H, Palamutcu S (2016) Functionalization of cotton fabric with nanosized TiO_2 coating for self-cleaning and antibacterial property enhancement. J Coat Technol Res 13(2):257–265. https://doi.org/10.1007/s11998-015-9743-7

Duraimurugan J, Shanavas S, Ramesh R, Acevedo R, Anbarasan P, Maadeswaran P (2020) Hydrothermal assisted phytofabrication of zinc oxide nanoparticles with different nanoscale characteristics for the photocatlytic degradation of Rhodamine B. Optik 202:163607. https://doi.org/10.1016/j.ijleo.2019.163607

Ekande OS, Kumar M (2021) Review on polyaniline as reductive photocatalyst for the construction of the visible light active heterojunction for the generation of reactive oxygen species. J Environ Chem Eng 9(4):105725. https://doi.org/10.1016/j.jece.2021.105725

El-Nahhal IM, Elmanama AA, Amara N, Qodih FS, Selmane M, Chehimi MM (2018) The efficacy of surfactants in stabilizing coating of nano-structured CuO particles onto the surface of cotton fibers and their antimicrobial activity. Mater Chem Phys 215:221–228. https://doi.org/10.1016/j.matchemphys.2018.05.012

Fan T, Hu R, Zhao Z, Liu Y, Lu M (2017) Surface micro-dissolve method of imparting self-cleaning property to cotton fabrics in NaOH/urea aqueous solution. Appl Surf Sci 400:524–529. https://doi.org/10.1016/j.apsusc.2016.12.184

Farouk A, Saeed SE-S, Sharaf S, Abd El-Hady M (2020) Photocatalytic activity and antibacterial properties of linen fabric using reduced graphene oxide/silver nanocomposite. RSC Adv 10(68):41600–41611. https://doi.org/10.1039/D0RA07544B

Feng J, Li J, Lv W, Xu H, Yang H, Yan W (2014) Synthesis of polypyrrole nano-fibers with hierarchical structure and its adsorption property of Acid Red G from aqueous solution. Synth Met 191:66–73. https://doi.org/10.1016/j.synthmet.2014.02.013

Franco FC (2020) Interaction of several toxic heterocarbonyl gases with polypyrrole as a potential gas sensor. Chemosensors 8(3):84. https://doi.org/10.3390/chemosensors8030084

Gao D, Wang L, Wang C, Chen T (2019) Photocatalytic self-cleaning cotton fabrics coated by Cu2 (OH) PO4 under VIS/NIR irradiation. Materials 12(2):238. https://doi.org/10.3390/ma12020238

Gómez-Velázquez LS, Madriz L, Rigoletto M, Laurenti E, Bizarro M, Dell'Arciprete ML, González MC (2023) Structural and physicochemical properties of carbon nitride nanoparticles via precursor thermal treatment: effect on methyl orange photocatalytic discoloration. ACS Appl Nano Mater. https://doi.org/10.1021/acsanm.3c01935

Hassabo AG, El-Naggar ME, Mohamed AL, Hebeish AA (2019) Development of multifunctional modified cotton fabric with tri-component nanoparticles of silver, copper and zinc oxide. Carbohydr Polym 210:144–156. https://doi.org/10.1016/j.carbpol.2019.01.066

Hebeish A, Abdelhady M, Youssef A (2013) TiO_2 nanowire and TiO_2 nanowire doped Ag-PVP nanocomposite for antimicrobial and self-cleaning cotton textile. Carbohydr Polym 91(2):549–559. https://doi.org/10.1016/j.carbpol.2012.08.068

Himmelsbach DS, Hellgeth JW, McAlister DD (2006) Development and use of an attenuated total reflectance/Fourier transform infrared (ATR/FT-IR) spectral database to identify foreign matter in cotton. J Agric Food Chem 54(20):7405–7412. https://doi.org/10.1021/jf052949g

Hoefer D, Hammer TR (2011) Antimicrobial active clothes display no adverse effects on the ecological balance of the healthy human skin microflora. Int Sch Res Notices. https://doi.org/10.5402/2011/369603

Hu R, Zhao Z, Zhou J, Fan T, Liu Y, Zhao T, Lu M (2019) Ultrasound assisted surface micro-dissolution to embed nano TiO_2 on cotton fabrics in $ZnCl_2$ aqueous solution. Ultrason Sonochem 56:160–166. https://doi.org/10.1016/j.ultsonch.2019.04.006

Hu X, Li Y, Xu Y, Gan Z, Zou X, Shi J, Li Y (2021) Green one-step synthesis of carbon quantum dots from orange peel for fluorescent detection of Escherichia coli in milk. Food Chem 339:127775. https://doi.org/10.1016/j.foodchem.2020.127775

Huang Z, Chen H, Zhao L, Fang W, He X, Li W, Tian P (2019) In suit inducing electron-donating and electron-withdrawing groups in carbon nitride by one-step NH_4Cl-assisted route: a strategy for high solar hydrogen production efficiency. Environ Int 126:289–297. https://doi.org/10.1016/j.envint.2019.02.030

Idris AO, Oseghe EO, Msagati TA, Kuvarega AT, Feleni U, Mamba B (2020) Graphitic carbon nitride: a highly electroactive nanomaterial for environmental and clinical sensing. Sensors 20(20):5743. https://doi.org/10.3390/s20205743

Jain R, Jadon N, Pawaiya A (2017) Polypyrrole based next generation electrochemical sensors and biosensors: a review. TrAC - Trends Anal Chem 97:363–373. https://doi.org/10.1016/j.trac.2017.10.009

Jeyasubramanian K, Hikku G, Preethi A, Benitha V, Selvakumar N (2016) Fabrication of water repellent cotton fabric by coating nano particle impregnated hydrophobic additives and its characterization. J Ind Eng Chem 37:180–189. https://doi.org/10.1016/j.jiec.2016.03.023

Ji X, Li H, Qin Y, Yan J (2022) Performance enhancement of self-cleaning cotton fabric with ZnO NPs and dicarboxylic acids. Crystals 12(2):214. https://doi.org/10.3390/cryst12020214

Jiang J et al (2014) Dependence of electronic structure of g-C_3N_4 on the layer number of its nanosheets: a study by Raman spectroscopy coupled with first-principles calculations. Carbon 80:213–221. https://doi.org/10.1016/j.carbon.2014.08.059

Jiang C, Liu W, Yang M, He S, Xie Y, Wang Z (2018) Synthesis of superhydrophobic fluoro-containing silica sol coatings for cotton textile by one-step sol–gel process. J Solgel Sci Technol 87:455–463. https://doi.org/10.1007/s10971-018-4750-7

Kang Y, Yang Y, Yin LC, Kang X, Liu G, Cheng HM (2015) An amorphous carbon nitride photocatalyst with greatly extended visible-light-responsive range for photocatalytic hydrogen generation. Adv Mater 27(31):4572–4577. https://doi.org/10.1002/adma.201501939

Krishnamoorthy K, Navaneethaiyer U, Mohan R, Lee J, Kim S-J (2012) Graphene oxide nanostructures modified multifunctional cotton fabrics. Appl Nanosci 2:119–126. https://doi.org/10.1007/s13204-011-0045-9

Lam S-M, Lim C-L, Sin J-C, Zeng H, Lin H, Li H (2021) Facile synthesis of MnO_2/ZnO coated on cotton fabric for boosted antimicrobial, self-cleaning and photocatalytic activities under sunlight. Mater Lett 305:130818. https://doi.org/10.1016/j.matlet.2021.130818

Liao J, Huang S, Ning C, Tan G, Pan H, Zhang Y (2013) Potential-induced reversible switching in the tubular structure of conducting polypyrrole nanotube arrays. RSC Adv 3(35):14946–14949. https://doi.org/10.1039/c3ra42172d

Luo Y, Yan Y, Zheng S, Xue H, Pang H (2019) Graphitic carbon nitride based materials for electrochemical energy storage. J Mater Chem A 7(3):901–924. https://doi.org/10.1039/C8TA08464E

Ma G, Wen Z, Wang Q, Shen C, Peng P, Jin J, Wu X (2015) Enhanced performance of lithium sulfur battery with self-assembly polypyrrole nanotube film as the functional interlayer. J Power Sources 273:511–516

Mahmoodi NM (2014) Binary catalyst system dye degradation using photocatalysis. Fibers Polym 15(2):273–280. https://doi.org/10.1007/s12221-014-0273-1

Maślana K et al (2020) Synthesis and characterization of nitrogen-doped carbon nanotubes derived from g-C3N4. Materials 13(6):1349. https://doi.org/10.3390/ma13061349

Meganathan P, Subbaiah S, Selvaraj LM, Subramanian V, Pitchaimuthu S, Srinivasan N (2022) Photocatalytic self-cleaning and antibacterial activity of cotton fabric coated with polyaniline/carbon nitride composite for smart textile application. Phosphorus Sulfur Silicon Relat Elem 197(3):244–253. https://doi.org/10.1080/10426507.2021.2012779

Ong W-J, Tan L-L, Ng YH, Yong S-T, Chai S-P (2016) Graphitic carbon nitride (g-C3N4)-Based photocatalysts for artificial photosynthesis and environmental remediation: are we a step closer to achieving sustainability? Chem Rev 116(12):7159–7329. https://doi.org/10.1021/acs.chemrev.6600075

Ovando-Medina VM, Dávila-Guzmán NE, Pérez-Aguilar NV, Martínez-Gutiérrez H, Antonio-Carmona ID, Martínez-Amador SY, Dector A (2018) A semi-conducting polypyrrole/coffee grounds waste composite for rhodamine B dye adsorption. Iran Polym J 27(3):171–181. https://doi.org/10.1007/s13726-018-0598-5

Özdemir AO, Caglar B, Çubuk O, Coldur F, Kuzucu M, Guner EK, Özdokur KV (2022) Facile synthesis of TiO2-coated cotton fabric and its versatile applications in photocatalysis, pH sensor and antibacterial activities. Mater Chem Phys. https://doi.org/10.1016/j.matchemphys.2022.126342

Pal S, Mondal S, Maity J (2018) Synthesis, characterization and photocatalytic properties of ZnO nanoparticles and cotton fabric modified with ZnO nanoparticles via in-situ hydrothermal coating technique: dual response. Mater Technol 33(14):884–891. https://doi.org/10.1080/10667857.2018.1521592

Peng Y, Qiu L, Pan C, Wang C, Shang S, Yan F (2012) Facile preparation of water dispersible polypyrrole nanotube-supported silver nanoparticles for hydrogen peroxide reduction and surface-enhanced Raman scattering. Electrochim Acta 75:399–405. https://doi.org/10.1016/j.optlastec.2019.105705

Praveen S, Sim GS, Ho CW, Lee CW (2021) 3D-printed twisted yarn-type Li-ion battery towards smart fabrics. Energy Storage Mater 41:748–757. https://doi.org/10.1016/j.ensm.2021.07.024

Ran J, Chen H, Bai X, Bi S, Jiang H, Cai G, Wang X (2019) Immobilizing CuO/$BiVO_4$ nanocomposite on PDA-templated cotton fabric for visible light photocatalysis, antimicrobial activity and UV protection. Appl Surf Sci 493:1167–1176. https://doi.org/10.1016/j.apsusc.2019.07.137

Sarwar N, Humayoun B, Dastgeer U, Yoon DH (2021) Copper nanoparticles induced, trimesic acid grafted cellulose: an effective, non-hazardous processing approach for multifunctional textile with low chemical induction. Cellulose 28:11609–11624

Sedighi A, Montazer M, Samadi N (2014) Synthesis of nano Cu_2O on cotton: morphological, physical, biological and optical sensing characterizations. Carbohydr Polym 110:489–498. https://doi.org/10.1016/j.carbpol.2014.04.030

Selvam S, Yim J-H (2023) Biocompatible and electrolyte embossed wearable textile based supercapacitors from chitosan derived bio-ternary composites crafted fabric electrodes. J Energy Storage 58:106340. https://doi.org/10.1016/j.est.2022.106340

Seth M, Jana S (2022) Green synthesis of hierarchically structured Ag–Cu_2O on cotton fabric with sustained antimicrobial activity and on-demand oil–water separation ability. Cellulose 29(8):4703–4724. https://doi.org/10.1007/s10570-022-04556-z

Shahbaz M, Urano S, LeBreton PR, Rossman MA, Hosmane RS, Leonard NJ (1984) Tri-s-triazine: synthesis, chemical behavior, and spectroscopic and theoretical probes of valence orbital structure. J Am Chem Soc 106(10):2805–2811. https://doi.org/10.1021/ja00322a014

Shahedifar V, Rezadoust AM (2013) Thermal and mechanical behavior of cotton/vinyl ester composites: effects of some flame retardants and fiber treatment. J Reinf Plast Compos 32(10):681–688. https://doi.org/10.1177/0731684413475911

Singh A, Salmi Z, Jha P, Joshi N, Kumar A, Decorse P, Gupta SK (2013) One step synthesis of highly ordered free standing flexible polypyrrole-silver nanocomposite films at air–water interface by photopolymerization. RSC Adv

3(32):13329–13336. https://doi.org/10.1039/C3RA40884A

Sricharussin W, Threepopnatkul P, Neamjan N (2011) Effect of various shapes of zinc oxide nanoparticles on cotton fabric for UV-blocking and anti-bacterial properties. Fibers Polym 12(8):1037–1041. https://doi.org/10.1007/s12221-011-1037-9

Tan L, Xu J, Zhang X, Hang Z, Jia Y, Wang S (2015) Synthesis of g-C3N4/CeO2 nanocomposites with improved catalytic activity on the thermal decomposition of ammonium perchlorate. Appl Surf Sci 356:447–453. https://doi.org/10.1016/j.apsusc.2015.08.078

Varesano A, Vineis C, Aluigi A, Rombaldoni F, Tonetti C, Mazzuchetti G (2013) Antibacterial efficacy of polypyrrole in textile applications. Fibers Polym 14(1):36–42. https://doi.org/10.1007/s12221-013-0036-4

Vasantharaj S, Sathiyavimal S, Saravanan M, Senthilkumar P, Gnanasekaran K, Shanmugavel M, Pugazhendhi A (2019) Synthesis of ecofriendly copper oxide nanoparticles for fabrication over textile fabrics: characterization of antibacterial activity and dye degradation potential. J Photochem Photobiol B 191:143–149. https://doi.org/10.1016/j.jphotobiol.2018.12.026

Wan J, Li H, Cai X, Yan J, Liao Y (2022) Developing the functional cotton fabric with N-halamine antibacterial structure based on DA/PEI. Cellulose 29(18):9953–9967. https://doi.org/10.1007/s10570-022-04876-0

Wang J, Wang S (2022) A critical review on graphitic carbon nitride (g-C3N4)-based materials: Preparation, modification and environmental application. Coord Chem Rev 453:214338. https://doi.org/10.1016/j.ccr.2021.214338

Wang X, Maeda K, Thomas A, Takanabe K, Xin G, Carlsson JM, Antonietti M (2009) A metal-free polymeric photocatalyst for hydrogen production from water under visible light. Nat Mater 8(1):76–80. https://doi.org/10.1149/MA2016-02/49/3647

Wilson J, Radhakrishnan S, Sumathi C, Dharuman V (2012) Polypyrrole–polyaniline–Au (PPy–PANi–Au) nano composite films for label-free electrochemical DNA sensing. Sens Actuators B: Chem 171:216–222. https://doi.org/10.1016/j.snb.2012.03.019

Wu J, Sun Y, Pei W-B, Huang L, Xu W, Zhang Q (2014) Polypyrrole nanotube film for flexible thermoelectric application. Synth Met 196:173–177. https://doi.org/10.1016/j.synthmet.2014.08.001

Xie J, Pan W, Guo Z, Jiao SS, Ping Yang L (2019) In situ polymerization of polypyrrole on cotton fabrics as flexible electrothermal materials. J Eng Fibers Fabr. https://doi.org/10.1177/1558925019827447

Xu L, Wang W, Yu D (2017) Preparation of a reactive flame retardant and its finishing on cotton fabrics based on click chemistry. RSC Adv 7(4):2044–2050. https://doi.org/10.1039/C6RA26075F

Yetisen AK, Qu H, Manbachi A, Butt H, Dokmeci MR, Hinestroza JP, Yun SH (2016) Nanotechnology in textiles. ACS Nano 10(3):3042–3068. https://doi.org/10.1021/acsnano.5b08176

Yuen C-WM, Yip J, Liu L, Cheuk K, Kan C-W, Cheung H-C, Cheng S-Y (2012) Chitosan microcapsules loaded with either miconazole nitrate or clotrimazole, prepared via emulsion technique. Carbohydr Polym 89(3):795–801. https://doi.org/10.1016/j.carbpol.2012.04.013

Yuzer B, Aydın MI, Con AH, Inan H, Can S, Selcuk H, Kadmi Y (2022) Photocatalytic, self-cleaning and antibacterial properties of Cu (II) doped TiO_2. J Environ Manage 302:114023. https://doi.org/10.1016/j.jenvman.2021.114023

Zeng Z, Quan X, Yu H, Chen S, Zhang Y, Zhao H, Zhang S (2018) Carbon nitride with electron storage property: enhanced exciton dissociation for high-efficient photocatalysis. Appl Catal 236:99–106. https://doi.org/10.1016/j.apcatb.2018.05.003

Zhu C, Shi J, Xu S, Ishimori M, Sui J, Morikawa H (2017) Design and characterization of self-cleaning cotton fabrics exploiting zinc oxide nanoparticle-triggered photocatalytic degradation. Cellulose 24:2657–2667. https://doi.org/10.1007/s10570-017-1289-7